Journal of Radiation and Nuclear Applications
An International Journal

http://dx.doi.org/10.18576/jrna/090208

Photon Shielding Capability of Concrete Doped with FeO for Radiotherapy Application

Adam I. Usman[1], Ibrahim G. Kefas[1], Musa Mohammed[2], Gimba A. Zephaniah[3], Alhaji S. Ismail[4], Akoso C. Christopher[1] and Idris M. Mustapha[1]*

[1]Department of Physics, Nasarawa State University, Keffi, Nasarawa State, Nigeria.
[2]Department of Physics, Modibbo Adama University, Yola, Adamawa State, Nigeria.
[3]Department of Radiology and Radiation Sciences, Bingham University, Karu, Nasarawa State, Nigeria.
[4]Department of Statistics, Nasarawa State University, Keffi, Nasarawa State Nigeria.

Received: 2 Feb. 2024, Revised: 22 March. 2024, Accepted: 1 April. 2024.

Published online: 1 May 2024

Abstract: This study investigates the photon shielding capability of concrete doped with FeO, photon attenuation parameters were determined for medical radiation application. The Win XCOM software was used to determine the mass attenuation coefficient (MAC) of the concrete doped FeO samples (0, 30, 50, 70, and 100 % FeO content) for the energy range (0.01-10.0 MeV). The linear attenuation coefficient(LAC), half value layer (HVL), tenth value layer (TVL), mean free path (MFP), and effective atomic number (Zeff) were calculated from the MAC values. The MAC values of the samples decrease rapidly up to 0.12 MeV, and beyond 0.12 MeV, Compton scattering becomes effective at intermediate energies. The LAC value varies with energy in a similar way as MAC. The calculated HVL and MFP were observed to decline as the FeO doping of the concrete increased which accounts for the three-photon interaction mechanisms' effectiveness in the variation of HVL and MFP values with energy. The Zeff shows minimal variation as the energy increases in all the concrete-doped FeO samples. The study indicates that the attenuation of shielding material can be significantly enhanced by FeO doping and can be deployed for medical radiation shielding applications.
Keywords: WinXCOM software, mass attenuation coefficient, gamma radiation, and radiation shielding.

1 Introduction

The continuous beneficial use of ionizing radiation (IR) and radioisotopes in the diagnosis and treatment of health trauma; electricity generation; food processing and preservation; material characterization and other peaceful purposes is hinged on adequate radiation protection of man and the biota against the harmful effect of IR [1]. The increased demand for ionizing radiation in many areas of endeavor such as radiotherapy is one of the most concerning subjects regarding the use of medical radiation [2]. Radiation shielding serves several functions; foremost among these is reducing the radiation exposure to persons in the vicinity of radiation sources. Shielding used for this purpose is named biological shielding [3- 5]. Standard materials such as lead and concrete have been used in shielding materials from ionizing radiation but have some limitations [6, 7]. As such, it is necessary to improve the attenuating properties of concrete by doping it with another material.

Traditionally, materials for photon attenuation are required to be of high density; on the other hand, fast neutron shields require low-density hydrogenous materials as moderators. Materials rich in elements such as (B, Eu, Pu, and Cd) have high neutron absorption cross-sections [8, 9].

2 Materials and Methods

In this study, gamma attenuation parameters of concrete doped FeO of various mixing ratios of FeO content consisting of 0%, 30%, 50%, 70%, and 100% mol, were determined and their application as shielding material was discussed. Theoretical mass attenuation coefficients (μm) of the glass mixtures were calculated for the chemical composition of the concrete doped FeO mixtures using Win XCOM software. The XCOM code is a database for calculating mass attenuation coefficients at different photon energies.

*Corresponding author e-mail: greatikemba@googlemail.com

The term of mass attenuation coefficient (μm) for the selected sample is expressed using the following Lambert-Beer law [10-11],

$$I = I_o e^{-(\mu/\rho)t} \quad (1)$$

where I and I_o are the intensity with absorber and intensity without absorber, respectively, t in g/cm^2, is the thickness of the sample, and μ in g/cm^2, is the mass attenuation coefficient. In addition, the MAC values of the cement-doped FeO samples under study were also obtained [2].

The mean free path (MFP) is the average distance taken by a moving particle between two consecutive collisions. The following equation can obtain MFP values;

$$MFP = \frac{1}{\mu} \quad (2)$$

Half value layer (HVL) of the materials is the thickness which reduces the incident photon intensity to fifty percent. The equation (3) is utilized to determine the HVL for the material [4].

$$HVL = \frac{0.693}{\mu} \quad (3)$$

where μ (cm^{-1}) denotes linear attenuation coefficient which is determined by the multiplication of the MAC value and density of the sample (ρ) [12-15].

The Z_{eff} values of materials have a strong energy dependence, which differs from the Z (atomic number) of individual elements (for example, Z is constant with changing E). In this study, equation 4 was used to calculate the Z_{eff} of the investigated glass mixtures.

$$Z_{eff} = \frac{\sum f_i A_i \left(\frac{\mu}{\rho}\right)_i}{\frac{\sum f_j A_j}{Z_j}\left(\frac{\mu}{\rho}\right)_j} \quad (4)$$

where Z_i ,f_i, and A_i, are the atomic number, molar fraction, and atomic mass of the elements inside the samples, respectively [16].

3 Results and Discussion

The molar volume and density of the concrete-doped FeO are shown in Table 1. The densities of the samples were varied depending on the proportion of additives (FeO). The density and molar volume of samples are increased with increments in FeO percentage. The high density of a material is important not only for the attenuation of photon radiation but also for reducing the thickness of the shielding material.

The mass attenuation coefficient (MAC) of the samples was measured for 0.01-10.0 MeV photon energies theoretically by using the WinXCOM program shown in Table 2. The result shows the highest and lowest attenuation coefficient in the pure FeO sample (T5) and pure concrete sample (T1) respectively. The values of the attenuation coefficient increase with increasing FeO concentration in all the samples and depend on both photon energy and chemical composition of samples. In the low energy region, since photoelectric cross section changes is proportional to Z^4 and inversely proportional to the incident photon energy as $E^{3.5}$. Mass attenuation values of the samples were decreased rapidly up to 0.12 MeV. Beyond 0.12 MeV, Compton scattering becomes effective at intermediate energies. Mass attenuation values of the samples are almost constant and zero due to the linear dependence of the cross-section of Compton scattering with atomic number Z.

The linear attenuation coefficient (LAC) was calculated from MAC and the density of the samples as a function of energy as depicted in Fig. 2. The LAC varies with energy in a similar way as MAC. The increase in density of the samples greatly affects the attenuation capability.

Table 1: Chemical compositions and densities of the Concrete doped FeO

S/N	Sample Code	Concrete (%)	FeO (%)	Density
1.	T1	100	0	2.83
2.	T2	70	30	3.14
3.	T3	50	50	3.38
4.	T4	30	70	3.71
5.	T5	0	100	3.99

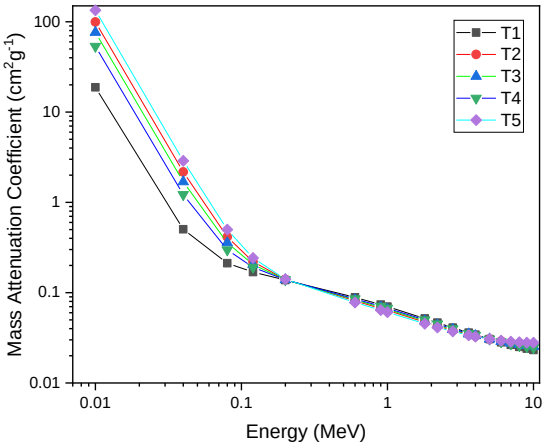

Fig. 1. Mass attenuation coefficient spectra of the concrete doped FeO samples.

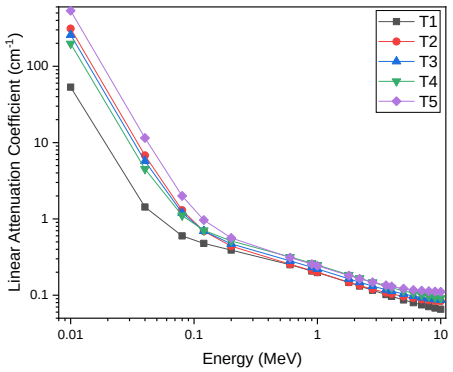

Fig. 2. Linear attenuation coefficient spectra of the concrete doped FeO samples.

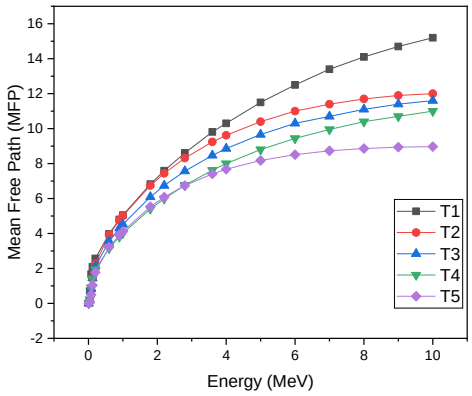

Fig. 4. Mean Free Path of the concrete doped FeO samples.

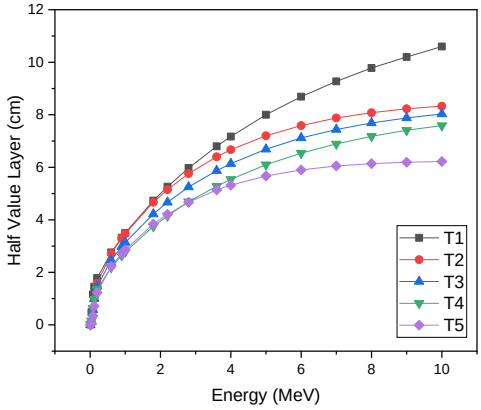

Fig. 3. Half Value Layer of the concrete doped FeO samples.

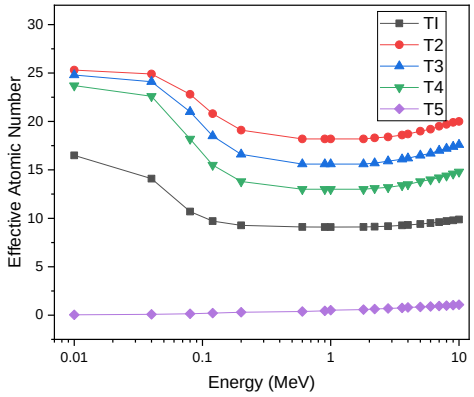

Fig. 5. Effective atomic number of the concrete doped FeO samples.

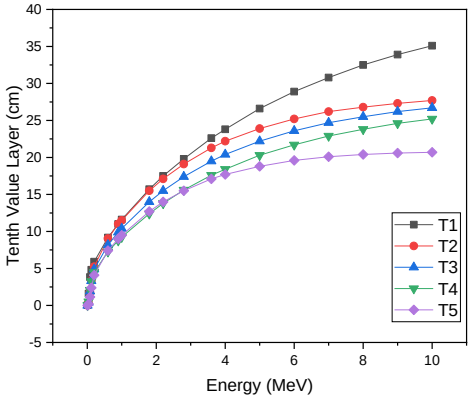

Fig. 3. Half Value Layer of the concrete doped FeO samples.

The half value layer (HVL), tenth value layer (TVL), and mean free path (MFP) enable us to obtain a material's shielding ability easily. Figures 3 and 4 represent HVL, TVL, and MFP values versus the incident photon energy for 0.01-10.0 MeV. In contrast to LAC values, HVL values are enhanced as the photon energy increases, respectively. The HVL, TVL, and MFP values also depend on the density of the sample in inverse proportion. Pure FeO samples have smaller values compared with other samples due to their higher density in both HVL, TVL, and MFP. Firstly, values of HVL and TVL were raised with increments in photon energy up to 2 MeV, then tended to rise slowly and remain stable. At low energies, HVL and TVL are less dependent on the content of the material.

A vital parameter to consider in a material to be substituted for radiation shielding is the effective atomic number (Z_{eff}). The fluctuation of Z_{eff} concerning photon energy is depicted in Fig. 5. The Z_{eff} of the samples shows a constant value

with negligible variation for all the concrete-doped FeO samples. The Pure concrete sample shows a drastic fall in Z_{eff} value to an energy of 0.04 MeV and flattens out for higher energy. The lower Z_{eff} values were found in low and high-energy regions for all samples. The addition of FeO in concrete systems is responsible for the increase in Z_{eff} values.

4 Conclusion

The research aimed to determine gamma ray shielding parameters of concrete doped FeO samples theoretically using WinXCOM software. The mass attenuation coefficient, linear attenuation coefficient, half value layer, tenth value layer, mean free path and effective atomic number, which are the significant gamma attenuation parameters were obtained theoretically for 0.01 – 10.0 MeV photon energies. The highest MAC and LAC values were observed at 10.0 MeV, i.e. low energies, for all the samples. In contrast to LAC values, HVL and TVL values are enhanced as the photon energy increases, respectively. The HVL, TVL, and MFP values also depend on the density of the sample in inverse proportion. The Z_{eff} of the samples shows a constant value with negligible variation for all the concrete-doped FeO samples. The Pure concrete sample shows a drastic fall in Z_{eff} value to an energy of 0.04 MeV and flattens out for higher energy. The outcomes indicate that the insertion of FeO into concrete enhanced the photon shielding parameters. It can be concluded that FeO-doped concrete samples can be further evaluated for gamma protection applications.

Reference

[1] Allam, EA., El-Sharkawy, RM., Shaaban, Kh. S., El-Taher, A., Mahmoud, ME., El Sayed, Y., Structural and thermal properties of nickel oxide nanoparticles doped cadmium zinc borate glasses: preparation and characterization Digest Journal of Nanomaterials & Biostructures (DJNB) 17 (1).2022.

[2] I. M. Mustapha, A. B. James, and S. M. Bello, “Photon Shielding Characterization of SiO2-PbO-CdO-TiO2 Glasses for Radiotherapy Shielding Application,” Asian J. Res. Rev. Phys., vol. 4, no. 4, pp. 32–38, 2021, doi: 10.9734/ajr2p/2021/v4i430150.

[3] Y. Kavun, H. Eskalen, and M. Kavgacı, “A study on gamma radiation shielding performance and characterization of graphitic carbon nitride,” J. Chem. Phys. Lett., vol. 811, no. 140246, 2023, [Online]. Available: https://doi.org/10.1016/j.cplett.2022.140246.

[4] Atef El-Taher., Hesham MH Zakaly., Mariia Pyshkina, EA Allam., R M El-Sharkawy, ME Mahmoud., Mohamed AE Abdel-Rahman., A comparative Study Between Fluka and Microshield Modelling Calculations to study the Radiation-Shielding of Nanoparticles and Plastic Waste Composites. Zeitschrift für anorganische und allgemeine Chemie 647 (10), 1083-1090. 202.

[5] H. Eskalen, Y. Kavun, S. Kerli, and S. Eken, “An investigation of radiation shielding properties of boron-doped ZnO thin films,” J. Opt. Mater., vol. 105, no. March, p. 109871, 2020, doi: 10.1016/j.optmat.2020.109871.

[6] A. El-Taher., H.M. Mahmoud, and Abbady, Adel G.E., Comparative Study of Attenuation and Scattering of Gamma –Ray through Two Intermediate Rocks. Indian Journal of Pure & Applied Physics, 45. 2007.

[7] Y.B, Saddeek., KH. S, Shaaban., R. Elsaman., A., El-Taher., T.Z Amer., Attenuation-density anomalous relationship of lead alkali borosilicate Glasses. Radiation Physics and Chemistry 150, 182–188. 2018.

[8] M. Afiq et al., “Recent Trends in Advanced Radiation Shielding Concrete for Construction of Facilities : Materials and Properties,” J. Polym., vol. 14, no. 1–47, 2022.

[9] Atef El-Taher., AM Ali., YB Saddeek., R. Elsaman., H Algarni., KS Shaaban., T.Z Amer., Gamma-ray shielding and structural properties of iron alkali alumino-phosphate glasses modified by PbO. Radiation Physics and Chemistry, 165, 108403. 2019.

[10] H. Al-ghamdi, M. Elsafi, A. H. Almuqrin, and S. Yasmin, “Investigation of the Gamma-ray Shielding Performance of CuO-CdO-Bi2O3 Bentonite Ceramics Hanan,” J. Mater., vol. 15, pp. 1–12, 2022.

[11] E. Kavaz, S. R. Armoosh, U. Peri, N. Ahmadi, and M. Oltulu, “Gamma-ray shielding effectiveness of the Portland cement pastes doped with brass-copper: An experimental study,” J. Radiat. Phys. Chem., vol. 166, no. July 2019, 2020, doi: 10.1016/j.radphyschem.2019.108526.

[12] EA Allam., RM El-Sharkawy., Atef El-Taher., ER Shaaban., EE Massoud., ME Mahmoud., Enhancement and optimization of gamma radiation shielding by doped nano HgO into nanoscale bentonite. Nuclear Engineering and Technology 54, 6, PP. 2253-2261. 2022.

[13] RM El-Sharkawy., EA Allam., Atef El-Taher., Reda Elsaman., EE Massoud., ME Mahmoud., Synergistic effects on gamma-ray shielding by novel light-weight nanocomposite materials of bentonite containing nano Bi2O3 additive. Ceramics International 48 (5), 7291-7303. 2022.

[14] RM El-Sharkawy., EA Allam., Atef El-Taher., E.R Shaaban, and ME Mahmoud., Synergistic Effect of Nano-bentonite and Nano cadmium Oxide Doping Concentrations on Assembly, Characterization and Enhanced Gamma-Rays Shielding Properties of

Polypropylene Ternary Nanocomposites. International Journal of Energy Research. 45 (6), 8942-8959. 2021.

[15] RM. El-Sharkawy., KS Shaaban., R. Elsaman., EA Allam., Atef El-Taher., ME Mahmoud., Investigation of mechanical and radiation shielding characteristics of novel glass systems with the composition xNiO-20ZnO-60B2O3-(20-x) CdO based on nanometal oxides. Journal of Non-Crystalline Solids. 528, 119754. 2020.

[16] ME Mahmoud., RM El-Sharkawy, EA Allam., R. Elsaman., Atef El-Taher., Fabrication and characterization of phosphotungstic acid-Copper oxide nanoparticles-Plastic waste nanocomposites for enhanced radiation-shielding. Journal of Alloys and Compounds 803, 768-777. 2019.